

Bose-Einstein condensation in a rotating anisotropic TOP trap

J. Arlt, O. Maragò, E. Hodby, S.A. Hopkins, G. Hechenblaikner, S. Webster and C.J. Foot.

Clarendon Laboratory, University of Oxford, Parks Road, Oxford, OX1 3PU, UK

Abstract. We describe the construction and operation of a time-orbiting potential trap (TOP trap) that has different oscillation frequencies along its three principal axes. These axes can be rotated and we have observed Bose-Einstein condensates of ^{87}Rb with a rotating ellipsoidal shape. Under these conditions it has been predicted that quantized vortices form and are stable.

PACS numbers: 03.75.Fi, 05.30.Jp, 32.80.Pj, 52.55.Lf

1. Introduction

The first experimental observations of Bose-Einstein condensation in alkali metals in 1995 [1, 2] and subsequent experiments have led to much progress, both theoretical and experimental, in understanding the physics of these condensed systems (for a review see [3]). Initial experiments focussed on the macroscopic properties of this new state of matter, such as collective excitations [4, 5]. Later experiments on atom lasers [6, 7] and the production of multi-component condensates [8, 9] have focussed on the coherence properties of BEC's. In particular the description of a condensate by a single wavefunction with a definite phase has been beautifully demonstrated by matter-wave interference experiments [10, 11]. Nevertheless, in contrast to earlier work on liquid helium [17], the spectacular phenomena of superfluidity have yet to be comprehensively demonstrated and studied in the alkali metal condensates e.g. non-viscous flow in narrow channels, quantised vortices and persistent currents. Some of these phenomena are a consequence of the irrotational nature of superfluid flow, which in turn stems from the existence of the single-valued wavefunction. Recently much theoretical effort, by various groups [12, 13, 14, 15, 16], has been devoted to possible methods of formation and observation of quantised vortices and persistent currents, which are associated with rotation of the condensate. It has been shown that rotating an anisotropic trap should create vortices in a similar manner to those observed in liquid helium [17].

In contrast to the time-averaged orbiting potential (TOP) trap used in this work, it is difficult to create a rotating potential using a magnetostatic trap such as the Ioffe-Pritchard [18] configuration. However it may be possible to study superfluidity

using other methods that have recently been suggested: stirring a trap with light forces [19], imprinting a 2π phase-winding with light beams [20] and manufacturing a vortical wavefunction in a spinor superposition state [21]. Only the latter method has been successful so far; the challenge of observing a vortex for a condensate in a single internal state has yet to be met.

However these alternative methods cannot directly test some of the interesting theoretical predictions which have recently been made for states in a rotating trap which have non-integer values of angular momentum (in units of Plancks constant) per particle [22]. The method presented here allows rotation without changing the ellipticity of the potential even for large ellipticities. These features cannot be achieved in the modulation method [4] used to excite $m = 2$ condensate excitations.

2. Experimental arrangement and BEC in TOP trap

We use a combination of laser cooling, magnetic trapping and evaporative cooling to obtain a ^{87}Rb condensate in the $F = 2, m_F = 2$ state in a similar manner to the first observation of BEC [1]. The experimental arrangement is similar to those described elsewhere [23, 24], and only important features of our setup are given below.

The light for our experiment comes from two external cavity diode lasers, *master* and *repumper*, operating close to the frequency of the rubidium D2-transitions. The light from the master laser is injected and amplified by a tapered semiconductor amplifier chip in a master oscillator power amplifier (MOPA) [25] configuration which provides ~ 500 mW of output. The light is fed to two magneto-optical traps (MOT) in a double trap configuration [26] to preserve a good vacuum in the experimental region while obtaining high loading rates.

A novel feature is the use of a pyramidal configuration of mirrors to form the collection MOT [27]. A large number of rubidium atoms are emitted from a getter source [28] in this region and then continuously cooled and transferred down a 30cm pipe of 15mm inner diameter, into the region of higher vacuum where they are captured in the second MOT. Magnetic guiding, in the transfer pipe, increases the flux of atoms to the second MOT by a factor of 2 [26]. The second MOT is a standard 6-beam MOT configuration used to capture and store the atoms. In order to obtain large numbers of atoms we found that it was beneficial to keep the small ($\approx 2G$) time-varying magnetic field used in the TOP trap switched on during loading into the second MOT. The Zeeman shift of this field causes atoms near the centre to be detuned from resonance, giving a partial dark MOT [29].

After collecting 5×10^8 atoms in the second MOT they are compressed, cooled to a temperature of $30\mu\text{K}$ in an optical molasses and then optically pumped into the $F = 2, m_F = 2$ state. The quadrupole field is created by two coils in anti-Helmholtz configuration with 500 turns each, operating at a maximum current of 10A. The 7kHz rotating field is created by two sets of Helmholtz coils with 5 turns in each coil. The current to each set of Helmholtz coils is supplied via matching transformers from a

600W audio amplifier.

Once the atoms are loaded into a mode-matched TOP trap (25G bias field and 65G/cm radial gradient) we use the following procedure to obtain BEC (see also Fig.1 (a)). Firstly the TOP and quadrupole fields are adiabatically ramped to 40G and 100G/cm in 2s to increase the collision rate. In a combined evaporation and compression ramp the radial quadrupole field gradient continues to rise to 194G/cm while the TOP field decreases to 20G in 20s. Now the TOP field itself is used to evaporate the hottest atoms by cutting to 1G in 28s obtaining a final radial trap frequency of $175Hz^\ddagger$. Finally a 5s radio frequency cut, finishing 60% of the way in from the radius of the locus of $B = 0$ ($\nu_{final} = 0.98MHz$), is used to obtain a pure condensate of $\sim 3 \times 10^4$ atoms. In Fig.1(a) it is possible to follow our path to BEC for ^{87}Rb in a phase space diagram and compare it with the case of ^{133}Cs [30] that has also been studied in a parallel experiment (using the same magnetic trap) at our lab [31].

The pictures in Fig.1(b) show the emergence of the pure condensate as the depth of the final RF cut is increased. We observe the sudden increase of optical depth and the reversal of shape characteristic for a BEC in time of flight (TOF) imaging. A laser pulse of $10\mu s$, synchronised with the TOP field and resonant with the $F = 2, m_F = 2 \rightarrow F' = 3, m'_F = 3$ transition, is used for absorption imaging of the cloud of atoms in the xz-plane.

3. Elliptical TOP potential

The invention of the TOP trap [23] lead to the first observation of BEC [1] in a dilute alkali vapour of rubidium, and this type of trap has subsequently also been used by other groups to trap caesium [31, 32] and sodium [7]. The TOP trap is formed by combining a spherical quadrupole field, which can be written as

$$\mathbf{B}_Q = B'_Q (x\mathbf{e}_x + y\mathbf{e}_y - 2z\mathbf{e}_z) \quad (1)$$

near the origin (B'_Q is the gradient), with a rotating field in the xy-plane

$$\mathbf{B} = B_x \cos \omega_0 t \mathbf{e}_x + B_y \sin \omega_0 t \mathbf{e}_y \quad (2)$$

The rotation frequency ω_0 is chosen to be greater than the oscillation frequencies of atoms in the trap ω_x, ω_y and ω_z , but less than the Larmor frequency so that atoms do not change m_F -state. The TOP trap is usually operated in the axisymmetric configuration where the amplitudes of the fields in the two directions are equal, $B_x = B_y$, and the trapping frequencies are in the ratios $\omega_x = \omega_y = \omega_z/\sqrt{8}$ §. However it is numerically straightforward to calculate the potential in the more general case where the ratio of the magnitudes of the rotating fields is $B_x/B_y = E$. The TOP potential is the time-average of

[‡] The trapping frequencies were measured by exciting 'dipole' oscillations of a small thermal cloud with a sudden change of the bias magnetic field.

§ A non axisymmetric TOP trap has been used to obtain BEC in Na [7].

$$U(x, y, z, t) = \mu B'_Q |(x + Er_0 \cos \omega_0 t) \mathbf{e}_x + (y + r_0 \sin \omega_0 t) \mathbf{e}_y - 2z \mathbf{e}_z| \quad (3)$$

where μ is the magnetic moment of the atoms and $r_0 = B_y/B'_Q$ is the distance from the centre of rotation at which the locus $B = 0$ intersects the y -axis. For $E = 1$ this locus is a circle of radius r_0 in the xy -plane, and in general it is an ellipse of eccentricity E in the xy plane described by the position vector

$$\mathbf{r} = r_0 (E \cos \omega_0 t \mathbf{e}_x + \sin \omega_0 t \mathbf{e}_y) \quad (4)$$

Without loss of generality we can consider $E \geq 1$ so that the order of the numerically calculated trapping frequencies, shown in Fig.2, is $\omega_x \leq \omega_y < \omega_z$. The harmonic approximation to the TOP potential

$$\bar{U} = \frac{1}{2} m (\omega_x^2 x^2 + \omega_y^2 y^2 + \omega_z^2 z^2) \quad (5)$$

is accurate at distances small compared to r_0 . We are mainly interested in the deformation of the time-averaged potential in the xy -plane, characterised by the parameter $\omega_y/\omega_x = e \geq 1$. Contours of constant energy in the xy -plane are ellipses given by

$$x^2 + e^2 y^2 = \text{constant} \quad (6)$$

whose major axes are in the same direction as the major axis of the ellipse in Eq. 3. Note however that the eccentricity of the TOP is much less than E and that the field in the x -direction reduces all the trap frequencies, not just ω_x . Thus it is not possible to reach very large deformations of the TOP potential. For small deformations the ellipticity in the trap frequency varies as $de/dE = 1/4$.

4. Rotation of the TOP

A rotation of an angle ϕ is mathematically obtained by a transformation of coordinates expressed by the matrix

$$\begin{pmatrix} \cos \phi & \sin \phi \\ -\sin \phi & \cos \phi \end{pmatrix}. \quad (7)$$

Applying this with a time varying angle $\phi = \Omega t$ to Eq.4 gives the position vector of a rotating ellipse

$$\begin{aligned} \mathbf{r}' &= r_0 (E \cos \Omega t \cos \omega_0 t + \sin \Omega t \sin \omega_0 t) \mathbf{e}_x + \\ &\quad r_0 (-E \sin \Omega t \cos \omega_0 t + \cos \Omega t \sin \omega_0 t) \mathbf{e}_y. \end{aligned} \quad (8)$$

When $E = 1$, this expression reduces to $\sin(\omega_0 - \Omega)t$ and $\cos(\omega_0 - \Omega)t$, which corresponds to the usual TOP configuration with a very slightly different frequency, since $\Omega \ll \omega_0$. (e.g. $\Omega \leq 2\pi \times 100 \text{ Hz}$ whereas $\omega_0 = 2\pi \times 7 \text{ kHz}$ in these experiments). To make the locus of $B = 0$ a rotating ellipse as described by Eq.8, we need to apply magnetic fields in the x and y directions which vary in time in the way described in these equations. This is achieved using the circuit shown schematically in Fig.3, starting with four signals proportional to $E \cos \omega_0 t$, $\sin \omega_0 t$, $\cos \Omega t$ and $\sin \Omega t$. These are then multiplied in pair by four voltage multiplier to give the four product voltages.

$$\begin{aligned}
A &= \cos \Omega t \, E \cos \omega_0 t \\
C &= \sin \Omega t \, \sin \omega_0 t \\
B &= \sin \Omega t \, E \cos \omega_0 t \\
D &= \cos \Omega t \, \sin \omega_0 t
\end{aligned} \tag{9}$$

These voltages are then added (or subtracted) by simple operational amplifier circuits to yield final signals

$$\begin{aligned}
B_x &\propto A + C \\
B_y &\propto D - B,
\end{aligned} \tag{10}$$

which are amplified by the audio amplifier and fed to the coils producing the time-varying fields along x and y.

It is important to ensure that any high frequency noise introduced in the multiplication and summing stages is filtered out before the amplifier otherwise it leads to a large decrease in the lifetime of the trapped atoms. This 'noise-induced' loss becomes more severe at lower values of the rotating bias field, and our present system cannot be operated below 1G.

5. BEC in the rotating anisotropic TOP trap

A simple description of the behaviour of trapped atoms in the elliptical rotating trap, is obtained from the classical equations of motion for anisotropic harmonic oscillation of a particle in a frame rotating at angular frequency Ω about the z-axis

$$\begin{aligned}
\ddot{x} &= -(\omega_x^2 - \Omega^2)x - 2\Omega \dot{y} \\
\ddot{y} &= -(\omega_y^2 - \Omega^2)y + 2\Omega \dot{x} \\
\ddot{z} &= -\omega_z^2 z
\end{aligned} \tag{11}$$

These equations are discussed in many mechanics textbooks e.g. in the book by Lamb [33], he shows that the two equations for the xy motion describe Blackburn's pendulum, a pendulum with different effective lengths in two orthogonal directions on a turntable. The oscillation frequencies in the x and y directions are reduced by the effect of the centripetal acceleration outwards and the x and y equations are coupled by the Coriolis force $\mathbf{\Omega} \times \dot{\mathbf{r}}$. One obvious feature of these equations is that the motion becomes unstable when the rotation is equal to the lowest trap oscillation frequency, $\Omega = \omega_x$.

We use the procedure outlined in section 2 to obtain a BEC in a normal circular TOP trap and then adiabatically change the amplitude of B_x , B_y or both to the desired ellipticity E . We found that the BEC remained condensed during this adiabatic expansion, during which the RF knife was switched off. Fig.4 shows time of flight images of the condensate after release from the rotating elliptical trap. By releasing the BEC when the probe beam was aligned with its long or its short axis the evolution of the x to z and y to z aspect ratios of the BEC was monitored. The inversion of the shape as the time of flight increases clearly demonstrates that the expansion of the cloud is dominated by its self energy. For the data shown in Fig.5 B_x remained at its

final value of $2G$ and B_y was ramped up to a value of $8G$ in $2s$ giving an ellipticity of the time-averaged potential of $E = 4$ and $e \approx 1.4$. These fields imply a static trap frequency of $70Hz$. With a rotation frequency of $30Hz$, one obtains an effective trap frequency $(\omega_x^2 - \Omega^2)^{1/2} = 63Hz$. We numerically solved the Castin-Dum [34] equations for the effective trap frequencies in a non-rotating frame. Fig.5 shows the comparison of experimental and theoretical data, which are in good agreement. This proves that our BEC has survived the rotation of the elliptical trap and that the Coriolis effects have had negligible influence.

6. Conclusions

We have constructed an anisotropic and rotating TOP trap and shown that a BEC may be created and transferred to the rotating trap. The measured properties at low rotation frequencies agree well with the existing theory. Faster rotation will be a useful tool for further studies of superfluid properties of a BEC, such as nucleation and stabilization of vortices.

We gratefully acknowledge fruitful discussions with J. Anglin, C. Clark, M. Edwards and D. Feder.

This work was supported by the EPSRC and the TMR program (No. ERB FMRX-CT96-0002). O. Maragò acknowledges the support of a Marie Curie Fellowship, TMR program (No. ERB FMBI-CT98-3077).

References

- [1] M.H. Anderson *et al.*, Science **269**, 198 (1995).
- [2] K.B. Davis *et al.*, Phys. Rev. Lett. **75**, 3969 (1995).
- [3] Proceedings of the International School of Physics 'Enrico Fermi' edited by M. Inguscio, S. Stringari and C.E. Wieman, in print (1998).
- [4] D.S. Jin *et al.*, Phys. Rev. Lett. **77**, 420 (1996).
- [5] M.-O. Mewes *et al.*, Phys. Rev. Lett. **77**, 988 (1996).
- [6] M.-O. Mewes *et al.*, Phys. Rev. Lett. **78**, 582 (1997).
- [7] E.W. Hagley *et al.*, Science **283**, 1706 (1999).
- [8] E.A. Cornett *et al.*, J. Low Temp. Phys. **113**, 151 (1998).
- [9] J. Stenger *et al.*, Nature **396**, 345 (1998).
- [10] M.R. Andrews *et al.*, Science **275**, 637 (1997).
- [11] B.P. Anderson *et al.*, Science **282**, 1686 (1998).
- [12] D.L. Feder *et al.*, Phys. Rev. Lett. **82**, 4956 (1999).
- [13] S. Stringari *et al.*, Phys. Rev. Lett. **82**, 4371 (1999).
- [14] A.A. Svidzinsky *et al.*, Phys. Rev. A **58**, 3168 (1998).
- [15] E. Lundh *et al.*, Phys. Rev. A **58**, 4816 (1998).
- [16] E.L. Bolda *et al.*, Phys. Rev. Lett. **81**, 5477 (1998).
- [17] D.R. Tilley and J. Tilley, "Superfluids and Superconductivity", Adam Hilger, (3rd ed 1991).
- [18] D.E. Pritchard *et al.*, Phys. Rev. Lett. **51**, 1336 (1983).
- [19] B.M. Caradoc-Davies *et al.*, Phys. Rev. Lett. **83**, 895 (1999).

- [20] R. Dum *et al.*, Phys. Rev. Lett. **80**, 2972 (1998).
- [21] M.R. Matthews *et al.*, Phys. Rev. Lett. **83**, 2498 (1999).
- [22] D.A. Butts *et al.*, Nature **397**, 327 (1999).
- [23] W. Petrich *et al.*, Phys. Rev. Lett. **74**, 3352 (1995).
- [24] J. Martin *et al.*, J. Phys. B **32**, 3065 (1999).
- [25] A. Wilson *et al.*, Appl. Opt. **37**, 4871 (1998).
- [26] C.J. Myatt *et al.*, Opt. Lett. **21**, 290 (1996).
- [27] J. Arlt *et al.*, Opt. Comm. **157**, 303 (1998).
- [28] C. Wieman *et al.*, Am. J. Phys. **63**, 317 (1995).
- [29] B.P. Anderson *et al.*, Phys. Rev. A **59**, R938 (1999).
- [30] S. Webster, D.Phil. thesis, Oxford University (to be published).
- [31] J. Arlt *et al.*, J. Phys. B **31**, L321 (1998).
- [32] M. Arndt *et al.*, Phys. Rev. Lett. **79**, 625 (1997).
- [33] H. Lamb, "Dynamics", Cambridge University Press (2nd ed 1923).
- [34] Y. Castin *et al.*, Phys. Rev. Lett. **77**, 5315 (1996).

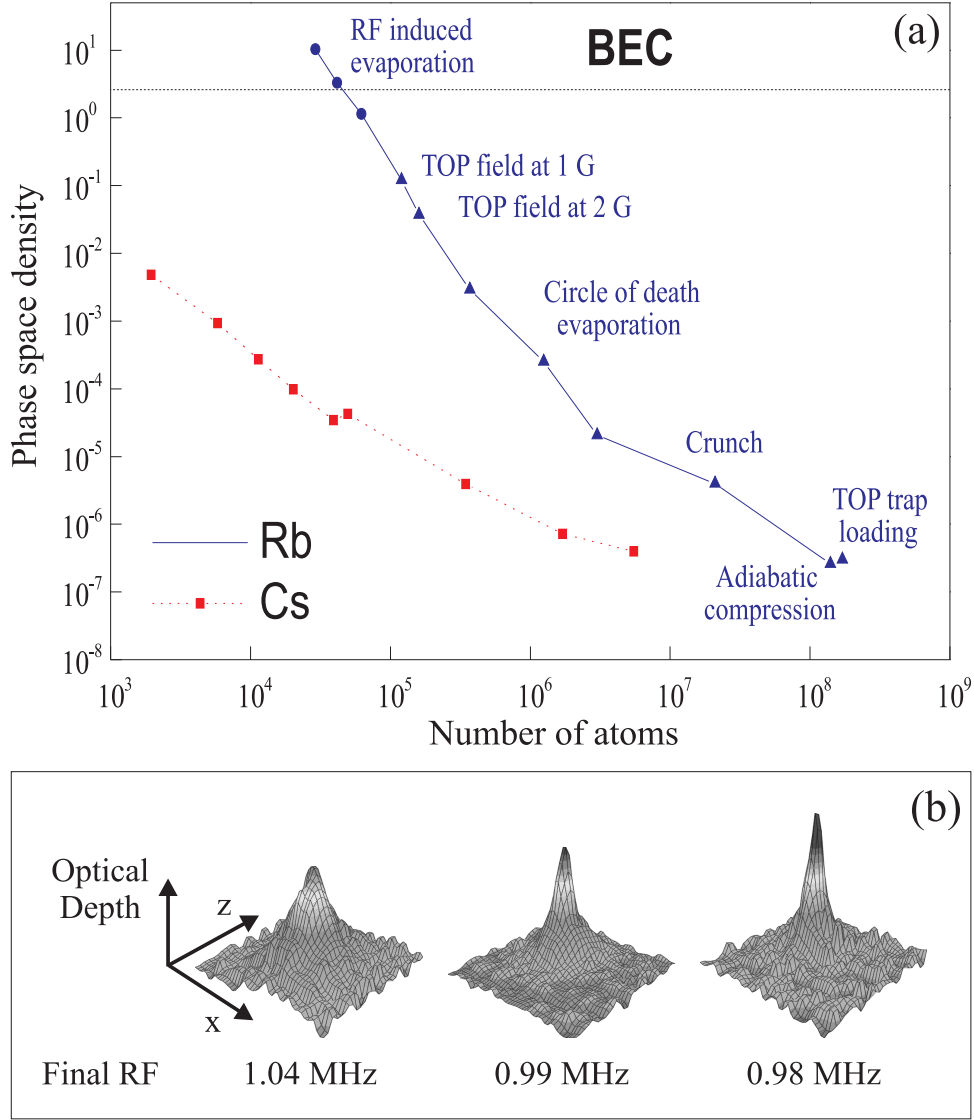


Figure 1. (a) Plot of phase space density vs. number of atoms during the evaporative cooling ramp. We compare the evaporative cooling efficiency for ^{87}Rb and ^{133}Cs in two identical magnetic traps. "Crunch" refers to the combined evaporation and compression ramp. (b) BEC formation in a trap with 1G bias field. The images were taken after 7ms TOF using absorption imaging.

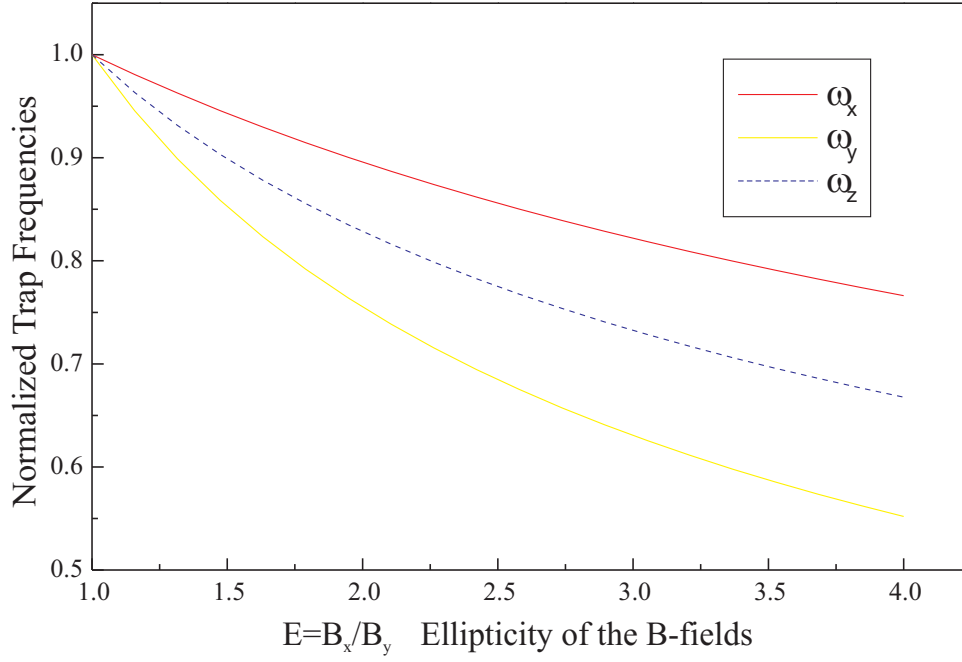


Figure 2. Plot of the trapping frequencies in an elliptical TOP trap as a function of the ellipticity $E = B_x/B_y$ where B_x is varying with E for fixed values of B_y and the quadrupole gradient. The frequencies are plotted as fractions of their values for $B_x = B_y$. The dotted line (ω_z) remains approximately equal to the mean of the other frequencies $(\omega_x + \omega_y)/2$.

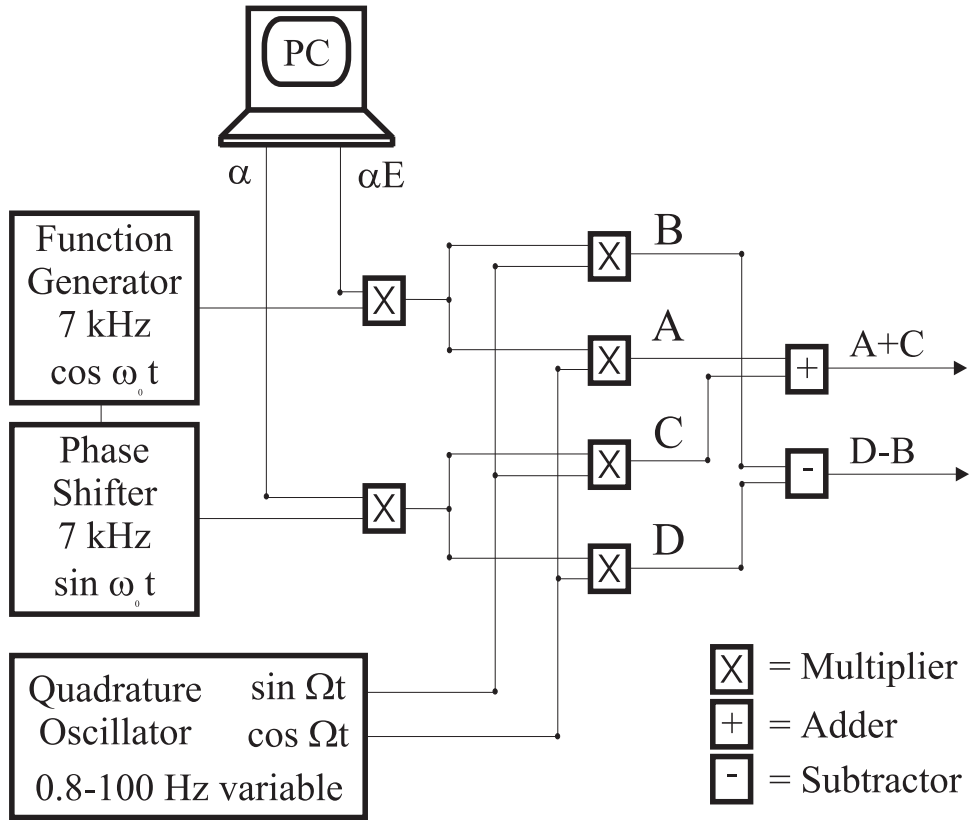


Figure 3. Schematic of the circuit for modulating the sine and cosine waves driving the TOP coils.

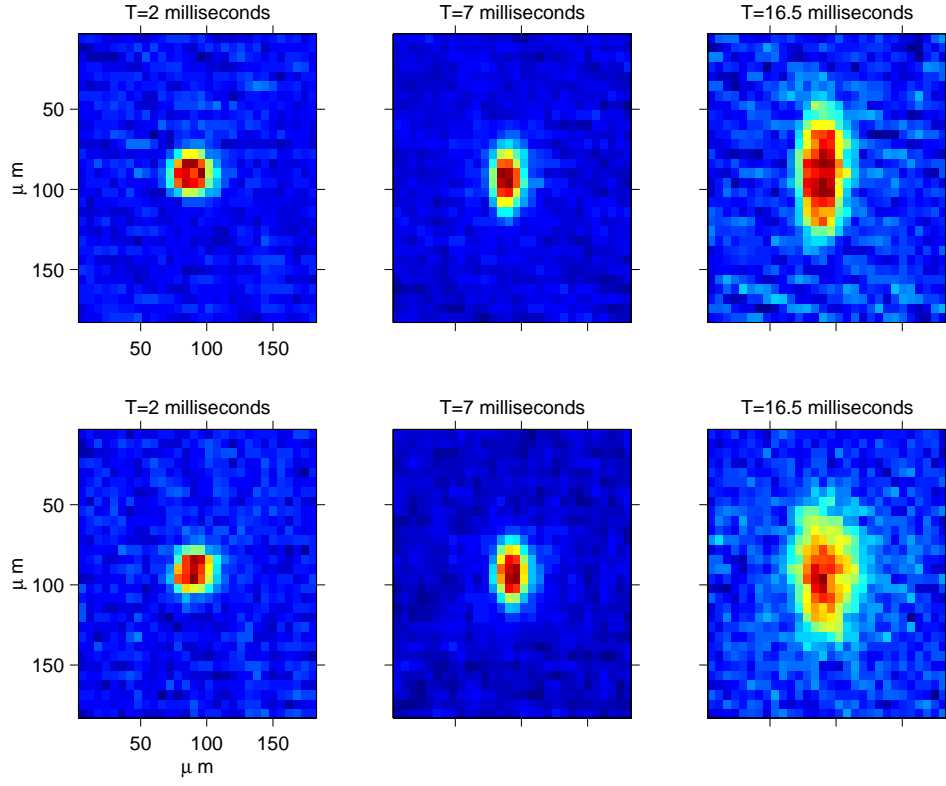


Figure 4. Pictures of BECs at different times of flight after being released from the elliptical rotating TOP trap. The top row shows BECs released with their x axes parallel to the imaging axes. The bottom row shows BECs released with their y axes parallel to the imaging axes.

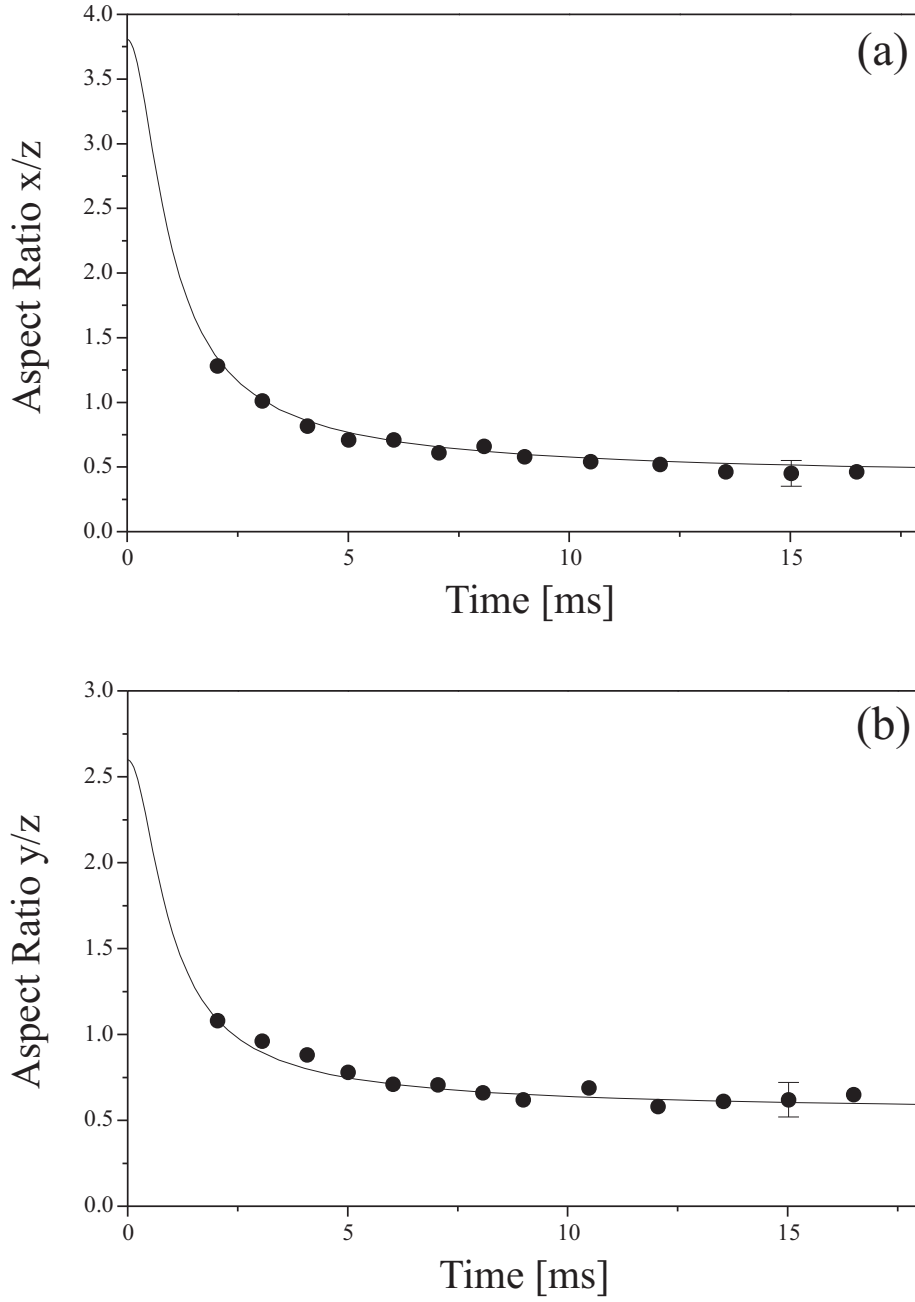


Figure 5. The expansion of the BEC is shown as a function of time. The aspect ratios evolve under the self-energy expansion. The theoretical curves have been obtained solving the Castin-Dum equations without free parameters. (a) Evolution of the x/z aspect ratio. (b) Evolution of the y/z aspect ratio. The data points are the average of four shots and the error bars represent their shot to shot variation.